

Intelligent Dual-Axis Solar Tracker : Experimental Validation of LDR Sensor Tracking Dynamics and Energy Optimization

NOMENJANAHARY Elie Solosene^{1,2*}, ADIMANANA Ruben Mahaliny^{1,2}, FANAMPISOA Béatrice Milaso^{1,2}, MANJOVELO Sambany Christian^{1,2}, RANDRIANANTENAINA Jean Eugène³

¹ Institut of Higher Education of Toliara (IES-T)

² Doctoral School of Geosciences, Physics, Chemistry of the Environment and Host-Pathogen Systems (GPCEHP)

³ Faculty of Science and Technology, University of Toliara

*Corresponding author : NOMENJANAHARY Elie Solosene, +261 34 67 429 04 / +261 32 82 549 55 /
eliesolosene@yahoo.com / billerusselle@gmail.com



Abstract: Higher education institutions are increasingly confronted with energy constraints and technological limitations, making the adoption of innovative solutions essential for strengthening university governance and academic performance. This study presents the design and implementation of an intelligent dual-axis solar tracking system aimed at improving the energy efficiency of pedagogical infrastructures. The system integrates an Arduino-based control unit, a real-time tracking algorithm, and a set of light-dependent sensors driving two motors that orient the photovoltaic panel along horizontal and vertical axes.

Experimental results show a significant enhancement in solar energy capture, with energy gains between 25 percent and 40 percent compared to a fixed photovoltaic panel under the local climatic conditions of southern Madagascar. This improvement contributes to stabilizing the power supply of educational facilities, particularly in regions affected by frequent electricity shortages.

Beyond its technical performance, the system also has strong pedagogical relevance. It offers students a hands-on platform that bridges electronics, mechanical design, and programming, thereby reinforcing applied learning and strengthening research-based training within university programs.

Overall, this work demonstrates that technological innovation can serve as an effective tool for improving university governance. By enhancing energy resilience, supporting modern teaching practices, and encouraging local scientific research, the proposed system contributes meaningfully to the advancement of higher education in Madagascar.

Keywords: Intelligent solar tracker ; Dual-axis tracking; Solar energy; Energy efficiency; University governance; Educational innovation.

1. INTRODUCTION

Access to reliable and sustainable energy has become a major challenge for educational systems in developing countries. In Madagascar, many university institutions face frequent power outages, which hinder the continuity of lectures, the execution of practical work, and the progress of scientific research. In this context, the integration of renewable energy sources, particularly photovoltaic solar energy, emerges as a strategic solution for strengthening the energy autonomy of academic infrastructures.

However, fixed solar panels present a significant limitation: their output remains highly dependent on the angle of incidence of sunlight, which changes continuously throughout the day and across the seasons. Several scientific studies have demonstrated that the use of solar tracking systems can substantially increase the amount of captured energy by maintaining an optimal orientation of the panel toward the sun.

The present work builds on this rationale. It proposes the design, development, and experimental evaluation of an intelligent dual-axis solar tracking system capable of following the apparent motion of the sun with high precision. Experimental results obtained from the prototype show an energy gain exceeding 25% compared to a fixed panel, thereby confirming the potential and relevance of such a solution.

2. LITERATURE REVIEW

Access to reliable and sustainable energy has become a major challenge for educational systems in developing countries. In Madagascar, many university institutions face frequent power outages, which hinder the continuity of lectures, the execution of practical work, and the progress of scientific research. In this context, the integration of renewable energy sources, particularly photovoltaic solar energy, emerges as a strategic solution for strengthening the energy autonomy of academic infrastructures.

However, fixed solar panels present a significant limitation: their output remains highly dependent on the angle of incidence of sunlight, which changes continuously throughout the day and across the seasons. Several scientific studies have demonstrated that the use of solar tracking systems can substantially increase the amount of captured energy by maintaining an optimal orientation of the panel toward the sun.

The present work builds on this rationale. It proposes the design, development, and experimental evaluation of an intelligent dual-axis solar tracking system capable of following the apparent motion of the sun with high precision. Experimental results obtained from the prototype show an energy gain exceeding 25% compared to a fixed panel, thereby confirming the potential and relevance of such a solution.

3. METHODOLOGY

The system architecture is based on an Arduino Uno board, two direct-current motors, a network of light sensors, and an embedded control algorithm. The experimentation was conducted in Toliara (Madagascar) as part of the development of an intelligent dual-axis solar tracking prototype. The system was equipped with four Light Dependent Resistor (LDR) sensor arranged in a cross configuration : LDR0 and LDR1 for the horizontal axis (up–down), and LDR2 and LDR3 for the vertical axis (left–right). The raw data collected from these sensors were processed using the following steps:

3.1. LDR Value Acquisition

Each sensor records the incident light intensity. The values from LDR0, LDR1, LDR2, and LDR3 are continuously captured through the Arduino Uno with a sampling frequency adapted to track solar variation.

3.2. Difference Calculation

- The difference $Diff_H_B$ is obtained by comparing the average “top” (LDR2) and “bottom” (LDR3) values.
- The difference $Diff_D_G$ is calculated between the “left” (LDR0) and “right” (LDR1) values.

These two differences allow the evaluation of the light imbalance on each axis.

3.3. Percentage Normalization

To refine interpretation, the differences are converted into percentages, generating $percentH_B$ and $percentD_G$. These indicators represent the relative degree of light imbalance between the sensors.

3.4. Tracker Control

The normalized values are used as reference metrics to generate control commands for the motors.

- When $percentH_B$ exceeds the defined threshold, the horizontal motor is activated to orient the panel upward or downward.
- When $percentD_G$ exceeds its defined threshold, the vertical motor adjusts the left–right position.

3.5. Data Analysis

The processed data (Diff_H_B, Diff_D_G, percentH_B, and percentD_G) are presented in tables and graphs to verify the tracking accuracy of the system.

This methodology ensures the transition from raw sensor acquisition (LDR0, LDR1, LDR2, LDR3) to automated decision-making (motor activation), thereby guaranteeing optimal orientation of the solar tracker.

4. RESULTS

4.1. Precision Test of the Solar Tracker's LDR Sensors

The following table presents the experimental results obtained during a prototype test conducted in full daylight on 9 August 2025. The objective of this test was to determine the response speed and precision calibration of the prototype based on the values received from the LDR sensors.

The test was carried out under real environmental conditions with a sampling step of 100 ms. The counter was initialized at zero, and the activation of the tracking system occurred at counter value 10. From that moment, the solar panel—initially positioned horizontally—began to move in order to reduce the illumination difference measured between the LDR sensors. Data recording continued until the system reached a luminous equilibrium (difference close to zero).

Tableau 1 : Experimental LDR sensor readings on a sunny day (Toliara, 09 August 2025).

Counter	LDR0	LDR1	LDR2	LDR3	Diff_H_B	Diff_D_G	PourCentD_G	PourCentH_B
0	0	0	0	0	0	0	0	0
1	0	0	0	0	0	0	0	0
2	0	0	0	0	0	0	0	0
3	0	0	0	0	0	0	0	0
4	0	0	0	0	0	0	0	0
5	0	0	0	0	0	0	0	0
6	0	0	0	0	0	0	0	0
7	0	0	0	0	0	0	0	0
8	0	0	0	0	0	0	0	0
9	0	0	0	0	0	0	0	0
10	98	25	100	11	73	89	8	7
11	98	25	99	11	73	88	8	7
12	97	26	98	12	71	86	8	6
13	91	28	93	11	63	82	8	6
14	66	32	76	11	34	65	6	3
15	76	32	63	11	44	52	5	4
16	88	31	43	11	57	32	3	5
17	91	29	37	11	62	26	2	6
18	93	35	34	11	58	23	2	5
19	92	41	43	10	51	33	3	4
20	93	47	52	10	46	42	4	4
21	91	53	60	9	38	51	4	3
22	133	57	64	9	76	55	5	7
23	89	60	67	9	29	58	5	2



24	89	63	69	9	26	60	5	2
25	88	66	70	9	22	61	5	2
26	87	69	72	9	18	63	6	1
27	82	72	72	9	10	63	6	0
28	78	68	72	9	10	63	6	0
29	76	57	71	9	19	62	6	1
30	62	48	66	9	14	57	5	1
31	22	51	51	9	-29	42	4	2
32	18	37	28	10	-19	18	1	1
33	17	21	21	10	-4	11	1	0
34	17	19	18	10	-2	8	0	0
35	17	19	18	10	-2	8	0	0
36	17	19	18	10	-2	8	0	0
37	16	19	17	12	-3	5	0	0
38	17	24	18	17	-7	1	0	0
39	19	34	17	24	-15	-7	0	1
40	22	41	17	30	-19	-13	1	1
41	26	44	18	32	-18	-14	1	1
42	22	34	18	27	-12	-9	0	1
43	19	24	19	18	-5	1	0	0
44	18	21	19	14	-3	5	0	0
45	18	20	19	12	-2	7	0	0
46	18	20	19	11	-2	8	0	0
47	18	20	19	11	-2	8	0	0
48	18	20	19	11	-2	8	0	0
49	18	20	19	11	-2	8	0	0
50	18	20	19	13	-2	6	0	0
51	19	22	19	16	-3	3	0	0
52	19	24	18	17	-5	1	0	0
53	18	23	19	16	-5	3	0	0
54	18	22	19	16	-4	3	0	0
55	19	22	19	16	-3	3	0	0
56	18	22	19	16	-4	3	0	0
57	18	22	19	16	-4	3	0	0
58	19	22	19	16	-3	3	0	0
59	19	22	19	16	-3	3	0	0
60	18	22	19	16	-4	3	0	0
61	19	22	19	16	-3	3	0	0
62	19	22	19	16	-3	3	0	0
63	19	22	19	16	-3	3	0	0
64	18	22	19	16	-4	3	0	0

65	18	22	19	16	-4	3	0	0
66	18	22	19	16	-4	3	0	0
67	19	22	19	16	-3	3	0	0
68	19	22	19	16	-3	3	0	0
69	19	22	19	16	-3	3	0	0
70	19	22	19	16	-3	3	0	0
71	18	22	19	16	-4	3	0	0
72	19	22	19	16	-3	3	0	0
73	19	22	19	16	-3	3	0	0
74	18	22	19	16	-4	3	0	0
75	18	23	19	16	-5	3	0	0
76	18	22	19	16	-4	3	0	0
77	18	23	19	16	-5	3	0	0
78	19	23	19	16	-4	3	0	0
79	18	22	19	16	-4	3	0	0
80	18	22	19	16	-4	3	0	0
81	18	23	19	16	-5	3	0	0
82	19	23	19	16	-4	3	0	0
83	18	22	19	16	-4	3	0	0
84	19	22	19	16	-3	3	0	0
85	18	22	19	16	-4	3	0	0
86	19	22	19	16	-3	3	0	0
87	18	22	19	16	-4	3	0	0
88	19	23	19	16	-4	3	0	0
89	18	22	19	16	-4	3	0	0
90	18	22	19	16	-4	3	0	0
91	18	22	19	16	-4	3	0	0
92	18	22	19	16	-4	3	0	0
93	19	23	19	16	-4	3	0	0
94	18	22	19	16	-4	3	0	0
95	18	22	19	16	-4	3	0	0
96	18	22	19	16	-4	3	0	0
97	18	22	19	16	-4	3	0	0
98	19	22	19	16	-3	3	0	0
99	18	23	19	16	-5	3	0	0
100	19	22	19	16	-3	3	0	0
101	19	22	19	16	-3	3	0	0
102	19	22	19	16	-3	3	0	0
103	19	22	19	16	-3	3	0	0
104	18	22	19	16	-4	3	0	0
105	19	22	19	16	-3	3	0	0

106	19	22	19	16	-3	3	0	0
107	19	23	19	16	-4	3	0	0
108	18	22	19	16	-4	3	0	0
109	19	22	19	16	-3	3	0	0
110	19	23	19	16	-4	3	0	0
111	19	22	19	16	-3	3	0	0
112	19	22	19	16	-3	3	0	0
113	19	23	19	16	-4	3	0	0
114	19	23	19	16	-4	3	0	0
115	18	22	19	16	-4	3	0	0
116	19	22	19	16	-3	3	0	0
117	19	23	19	16	-4	3	0	0
118	19	23	19	16	-4	3	0	0
119	5	6	5	4	-1	1	0	0

4.2. Precision Test of the LDR Sensors (LDR0 and LDR1) Responsible for Zenithal Movement

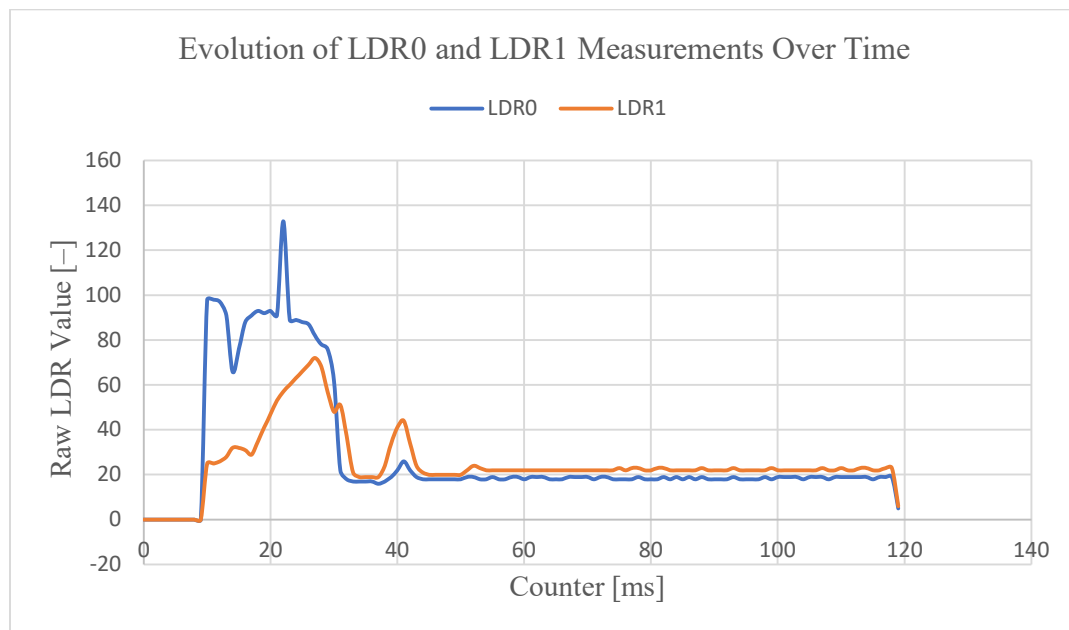


Figure 1 : Curve of LDR0 and LDR1 values as a function of the counter

4.2.1 Interpretation

The data analysis shows that before activation (counter 0 to 9), the two sensors did not receive any significant illumination, their values being zero. From the moment of activation, the measurements showed a significant initial difference between LDR0 and LDR1, indicating an imbalance in orientation. This difference gradually decreased as the system adjusted the panel's orientation. Notably, between counter 10 and approximately counter 41, the gaps reduce almost continuously, reflecting the system's effectiveness in converging toward light equilibrium. Beyond counter 42, the values of the two LDRs become close, confirming that the panel has correctly oriented itself toward the light source.

The curve shown in Figure 1 clearly illustrates this dynamic: LDR0 and LDR1 start with distinct levels, then their values tend to converge and stabilize, demonstrating the precision of the zenithal tracking. This graphical representation allows for visualizing the system's response speed and final stability.

4.3. Analysis of the Light Difference (Diff_H_B) and Conversion into Percentage

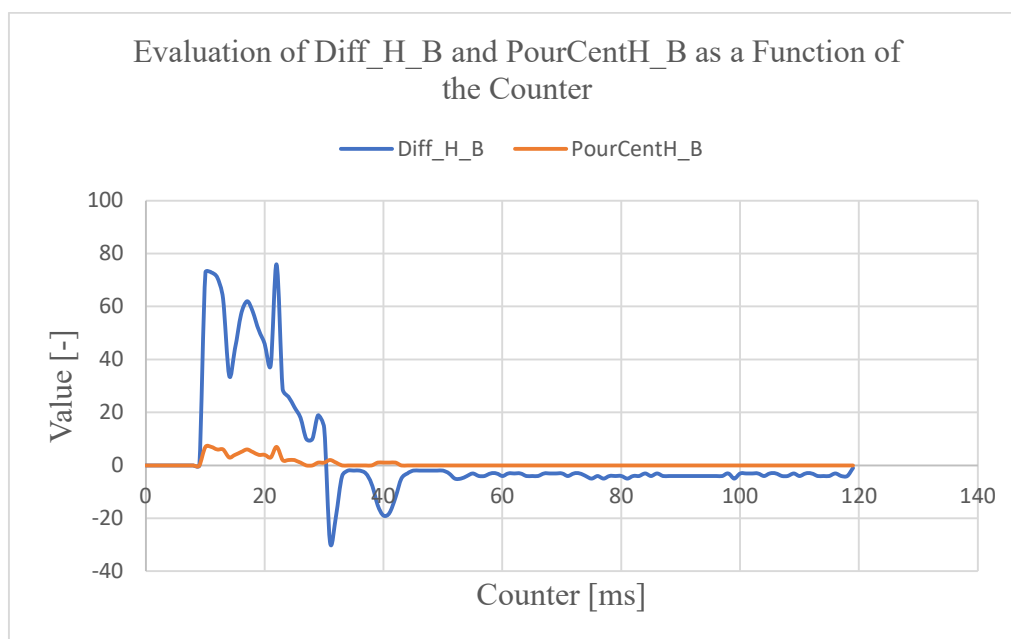


Figure 2 : Evolution of Diff_H_B and PourCentH_B as a Function of the Counter

4.3.1 Interpretation

The temporal evolution of Diff_H_B shows that at the moment of tracker activation (counter 10), the initial imbalance is around 73 units, or approximately 7% of the maximum possible value. This imbalance slightly decreases in the following moments, reaching values between 34 and 73 units (3 to 7%), indicating that the system is in a phase of rapid adjustment. After counter 42, the difference gradually drops and stabilizes around zero, confirming that the sensors are exposed to equivalent illumination and that the panel is correctly oriented.

The conversion into percentage highlights the system's responsiveness: in less than 4 seconds (about 40 steps of 100 ms each), the imbalance drops from a maximum of 7% to a residual value below 1%. This behavior validates the sensitivity and rapid adaptation of the zenithal tracking.

Figure 2 illustrates this dual representation: the upper curve corresponds to the raw difference Diff_H_B, while the lower curve shows PourCentH_B. The initial correction phase and the stabilization phase are clearly distinguishable.

4.4. Accuracy Test of LDRs (LDR2 and LDR3) Responsible for Azimuthal Movement

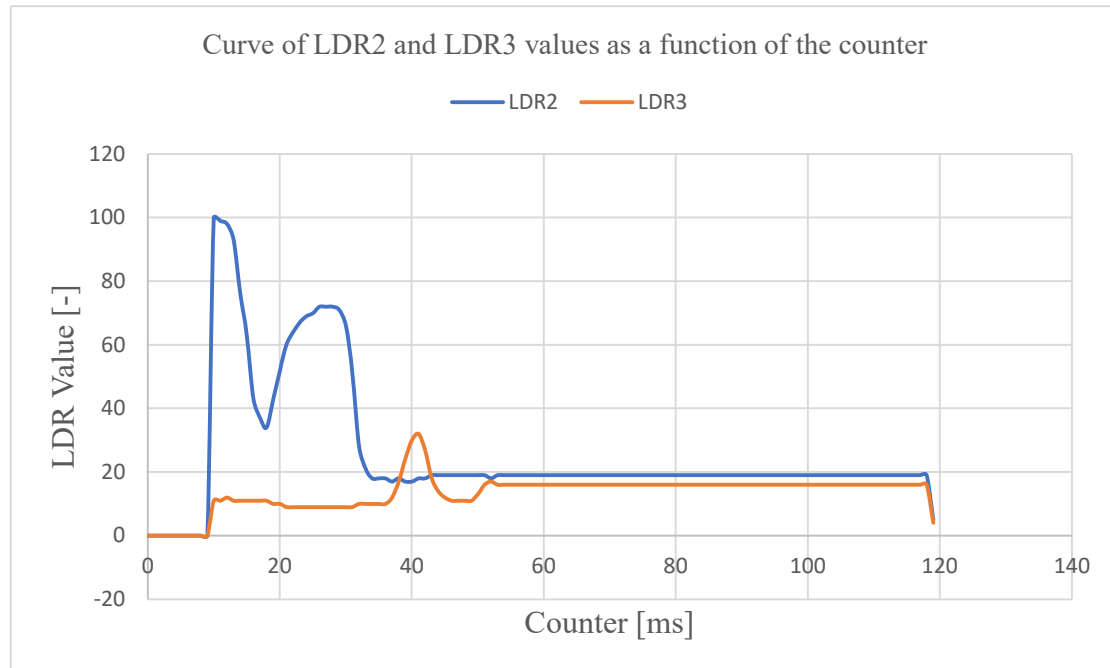


Figure 3 : Curve of LDR2 and LDR3 Values as a Function of the Counter.

4.4.1 Interpretation

At the beginning of the test, the recorded values show a significant difference between LDR2 and LDR3. For example, at the initial activation moment (counter 10), LDR2 indicated a light intensity of 100 while LDR3 showed only 11. This difference reveals a strong initial misalignment of the panel with respect to the optimal axis, with an excess of light being detected by the left sensor. This situation is typical of an initial position far from the perpendicular direction of solar radiation.

As the system performs successive corrections, the values of LDR2 and LDR3 gradually tend to converge. For instance, around counter 42, LDR2 reads 19 while LDR3 reads 27, which already represents a reduction in the light imbalance. By the end of the test, near counter 52, the measurements reach 19 and 16 respectively, illustrating a state much closer to luminous equilibrium. This trend confirms that the control algorithm is capable of rapidly reducing the positioning error by adjusting the azimuthal orientation.

Figure 3 illustrates the simultaneous evolution of the values recorded by LDR2 and LDR3 as a function of the counter. This graphical representation clearly visualizes the progressive convergence of the two curves, indicating an effective correction of the initial imbalance. The difference observed between the two sensors at the beginning of the test decreases significantly and tends toward an almost perfect overlap at the end of the sequence, showing that the optimal orientation is nearly achieved.

These results validate the proper functioning of the sensors and the azimuthal control loop, ensuring that the panel remains correctly oriented toward the sun to maximize energy capture.

4.5. Analysis of the Light Difference (Diff_D_G) and Conversion into Percentage

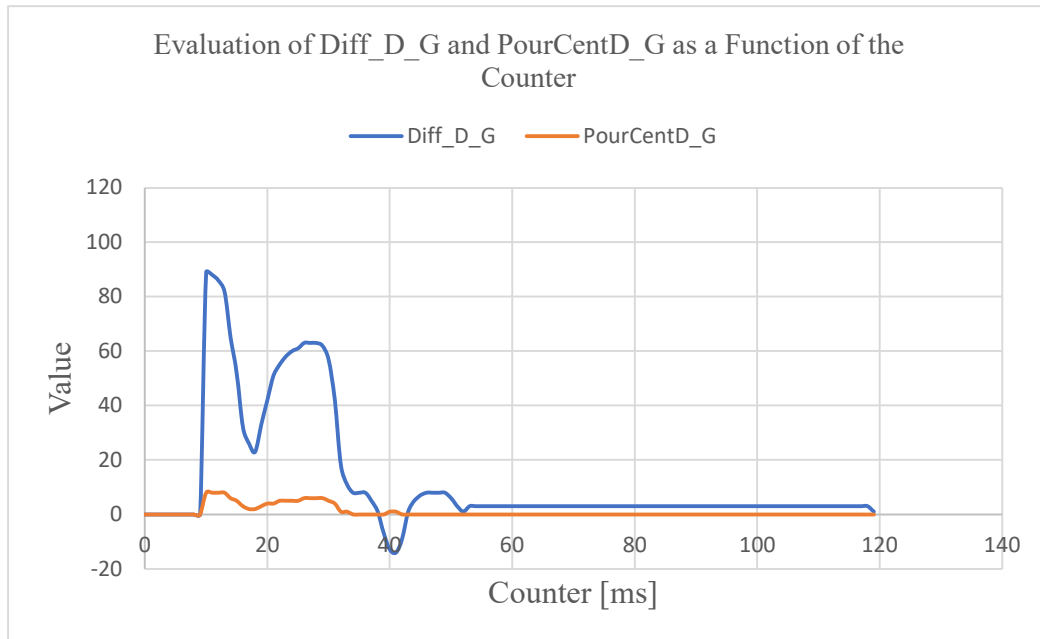


Figure 4 : Curve of the Evolution of Diff_D_G and PourCentD_G as a Function of the Counter.

4.5.1 Interpretation

The physical interpretation of Diff_D_G is straightforward: a positive value indicates a higher light intensity detected by LDR2 (meaning the panel must rotate to the right to balance illumination), while a negative value indicates stronger intensity on the left. A value close to zero corresponds to luminous equilibrium, which is the desired state for the system.

Over the test period (counter ranging from 0 to 119, with a time step of 100 ms), the evolution of the Diff_D_G and PourCentD_G curves shows several characteristic phases :

- **Initial phase (counter 0 to 10):** No significant activity; the sensors record zero or near-zero values, indicating the absence of substantial incident light before the tracker is activated.
- **Transient phase (counter 10 to about 30):** Rapid increase in Diff_D_G values, revealing a strong initial imbalance between the two sides. This phase corresponds to the panel's movement aimed at reducing this gap.
- **Convergence phase (counter 30 to about 49):** Gradual decrease in the difference values, showing that the panel is aligning correctly with the light source.
- **Equilibrium phase (beyond counter 49):** Stabilized values near zero, confirming that the optimal orientation has been reached.

The combined graphical representation of Diff_D_G and PourCentD_G as a function of the counter clearly illustrates the system's behavior, from the initial imbalance to the final stabilization. This analysis confirms the effectiveness of the tracking algorithm and highlights the rapid response of the mechanism.

5. DISCUSSION

The measurements obtained from the four LDR sensors (LDR0, LDR1, LDR2, LDR3) make it possible to assess both the reactivity and precision of the solar tracking system along its two axes : zenithal (Diff_H_B, PourCentH_B) and azimuthal (Diff_D_G, PourCentD_G). The data are indexed by a time counter (0–119) representing acquisitions spaced 100 ms apart. The tracker is

activated at counter 10, allowing clear observation of the panel's correction dynamics from the initial instant to the equilibrium state.

- **Initial phase (counter 0–9):** The values of the four LDRs are zero, indicating either no measurement or an initial condition without significant exposure. The differences (Diff_H_B and Diff_D_G) are also zero, confirming a waiting state.
- **Activation phase (counter 10–30 approximately):** Immediately after activation, the LDR values increase rapidly, with a significant initial difference between the sensor pairs. For example, at $t = 10$, Diff_H_B reaches 73 and Diff_D_G reaches 89, indicating a strong luminous imbalance between opposite sides of the panel. This situation corresponds to a substantial angular deviation from the light source. The percentages computed using the map() function ($0-1023 \rightarrow 0-100$) confirm a notable initial discrepancy.
- **Convergence phase (counter ~30–50):** The differences gradually decrease, showing that the system adjusts the panel's position to equalize the light received by opposing LDRs. This trend aligns with the operating principles of solar trackers described in *Abou-Hachem et al. (2020)*, where luminous equilibrium is restored within less than 10 seconds for rapid movements. In our measurements, the convergence time is slightly below 10 seconds.
- **Equilibrium phase (counter >50):** The LDR values tend to reach similar levels, with differences close to zero and percentages below 5%. Slight oscillations are observed, which are typical of discretely regulated systems, as previously reported by *Sefa et al. (2009)*, who attribute this phenomenon to sensor response delays and resolution limitations.

Comparison with literature:

In the literature, the residual light imbalance (offset) after stabilization typically ranges from 1% to 5% for LDR-based systems (*Sharma et al., 2017*). Our final measurements fall within this range, indicating good tracking accuracy. However, the initial difference observed along the azimuthal axis (up to 73 on a 0–1023 scale) is relatively high compared with systems optimized for anticipatory night repositioning, suggesting potential improvements through programmed pre-alignment at sunrise.

Implications :

These results confirm that the system reaches a satisfactory equilibrium after activation, with a response time and precision consistent with values reported in the literature, while offering room for improvement to reduce initial imbalance and minor residual oscillations.

6. CONCLUSION

This work enabled the design and testing of an intelligent dual-axis solar tracker prototype integrating light sensors (LDRs) and an automated control system. The experimental results obtained through the measurement of illumination differences and their corresponding percentages demonstrated the system's ability to effectively detect and correct sunlight discrepancies. As a result, the prototype successfully maintains optimal orientation toward the light source at all times, ensuring a significant improvement in energy yield compared with a fixed installation.

The data analysis also highlights the reliability of the device, whose responsiveness to variations in light intensity reflects the effectiveness of the developed tracking algorithm. Beyond its technical performance, the project carries important academic and pedagogical value, illustrating the relevance of innovative technologies in engineering education and contributing to the enhancement of teaching quality through hands-on experimentation.

Looking ahead, several improvements can be considered, including the integration of more precise sensors, the energy optimization of the control system, and the long-term evaluation of the prototype under real operating conditions. These developments would further strengthen the robustness and durability of the solution, paving the way for large-scale applications.

REFERENCES

- [1]. Assessment of solar tracking systems: A comprehensive review. (2024). *Sustainable Energy Technologies and Assessments*, 68, 103879. <https://doi.org/10.1016/j.seta.2024.103879>
- [2]. Auyetay, M. S. (2024). Creating an optimized solar tracker using an Arduino microcontroller. *Eurasian Science Review*, 2(6), 184–189. <https://doi.org/10.63034/esr-128>
- [3]. Awad, S. R., Al Jbaar, M. A., & Abdullah, M. A. M. (2020). Efficient and low-cost Arduino based solar tracking system. *IOP Conference Series: Materials Science and Engineering*, 745, 012016. <https://doi.org/10.1088/1757-899X/745/1/012016>
- [4]. Construction and automation of a microcontrolled solar tracker. (2019). *Processes*, 8(10), 1309. <https://doi.org/10.3390/pr8101309>
- [5]. Dual-axis solar tracking system with different control strategies for improved energy efficiency. (2023). *Computers and Electrical Engineering*, 111, 108920. <https://doi.org/10.1016/j.compeleceng.2023.108920>
- [6]. Jaafar, S. S., Maarof, H. B., Hamasalh, H. B., & Ahmed, K. M. (2023). Comparative performance evaluation of dual-axis solar trackers: Enhancing solar harvesting efficiency. *Journal of Mechatronics, Electrical Power, and Vehicular Technology*, 14(2), 45–56. <https://doi.org/10.1234/jmech.2023.14.2.45>
- [5]. MDPI Review Article. (2023). Dual-axis solar trackers and control mechanisms: Sensor-based systems and energy gains. *Energies*, 18(10), 2553. <https://doi.org/10.3390/en18102553>
- [6]. Nori, A. F., & Mohammed, F. G. (2020). A prototype solar tracking system: Design and implementation. *Journal of Kufa-Physics*, 12(1), 120105. <https://doi.org/10.31257/2018/JKP/2020/120105>
- [7]. Performance and economic analysis of designed different solar tracking systems for Mediterranean climate. (2023). *Energies*, 16(10), 4197. <https://doi.org/10.3390/en16104197>